Journal of Sound and Vibration (1996) **196**(4), 453–468

THE APPLICATION OF THE IRS AND BALANCED REALIZATION METHODS TO OBTAIN REDUCED MODELS OF STRUCTURES WITH LOCAL NON-LINEARITIES

M. I. Friswell

Department of Mechanical Engineering, University of Wales Swansea, Singleton Park, Swansea SA2 8PP, Wales

AND

J. E. T. Penny and S. D. Garvey

Department of Mechanical and Electrical Engineering, Aston University, Birmingham B4 7ET, England

(*Received 2 August* 1995, *and in final form* 17 *April* 1996)

This paper is concerned with the application of model reduction methods, which are popular for linear systems, to systems with local non-linearities, modelled by using finite element analysis. In particular these methods are demonstrated by obtaining the receptance of a continuous system with cubic stiffening discrete springs using the harmonic balance method. The model reduction methods available and the choice of master coordinates are considered. In the IRS method there is a conflict in the choice of master co-ordinates between the demands in the modelling of the non-linearity and the accuracy of the linear reduction. Other reduction methods considered are the reduction to modal co-ordinates and a balanced realization approach. Reduction to modal co-ordinates is easy to apply and gives acceptable results, although a more accurate reduced model may be obtained with IRS and the best choice of master co-ordinates. Reduction based on observability and controllability considerations, via balanced realizations, gives the most accurate reduced model. The reduction methods were compared in a time domain analysis by calculating the Poincaré map of a pinned beam with clearance. The balanced realization approach gave more accurate results than the reduction to modal co-ordinates for these simulations.

1. INTRODUCTION

The analysis of non-linear models with a large number of degrees-of-freedom requires considerable computational effort and therefore models of non-linear systems are generally restricted to a low number of degrees-of-freedom. In structural dynamics, finite element analysis is often used to obtain accurate discretized models of continuous systems, usually with hundreds if not thousands of degrees-of-freedom. If a non-linear component, for example a joint or a crack [1, 2], is added to the finite element model, then the calculation of the system response will require considerable computation. Non-linearities in these large models are often local in the sense that the forces in the non-linear components may be determined by a small number of degrees-of-freedom. In this paper the number of degrees-of-freedom in the model will be reduced by using a variety of methods thus speeding up the computation. Friswell *et al*. [3] introduced the idea of using reduction

0022–460X/96/390453 + 16 $18.00/0

based on the linear model but did not discuss the choice of retained co-ordinates in any detail.

Model reduction has considerable potential in substructuring. In linear systems, substructuring has been used to replace the solution of a large eigenproblem with the solutions of several smaller eigenproblems. Substructuring methods have been used to some extent in non-linear analysis [4, 5], although the number of degrees-of-freedom in the linear parts of the substructures would have to be reduced to realize fully the potential of substructuring.

2. USING MODEL REDUCTION FOR NON-LINEAR EQUATIONS

To obtain the receptance of a non-linear structure modelled with a large number of degrees-of-freedom requires the solution of a large number of non-linear differential equations. If a structure has only local non-linearities then it is possible to restrict the number of non-linear equations that need to be solved and obtain the receptance for the generalized co-ordinates from the reduced transformation.

Suppose the ordinary differential equation for the non-linear structure may be written in terms of the n-degrees-of-freedom $\mathbf{x}$ as

$$\mathbf{M}\ddot{\mathbf{x}} + \mathbf{D}\dot{\mathbf{x}} + \mathbf{K}\mathbf{x} + \mathbf{H}\mathbf{N}(\mathbf{x}) = \mathbf{B}\mathbf{f}(t), \qquad \mathbf{y} = \mathbf{C}\mathbf{x}, \tag{1}$$

where $\mathbf{M}$, $\mathbf{D}$ and $\mathbf{K}$ are the usual mass, damping and stiffness matrices, $\mathbf{f}$ is the applied force and $\mathbf{N}$ contains the non-linear terms. The matrices $\mathbf{H}$ and $\mathbf{B}$ distribute the non-linear terms and the applied force to the correct degrees-of-freedom. These matrices are not strictly necessary but their inclusion means that the non-linear force vector, $\mathbf{N}$, and the forcing vector, $\mathbf{f}$, have smaller dimensions. The measured degrees-of-freedom, $\mathbf{y}$, are determined by the matrix $\mathbf{C}$. Note that $\mathbf{D}$ is used for damping to allow control notation to be applied to the input and output matrices. If the non-linearity is local then it may be written in terms of a limited number of the generalized co-ordinates. Let

$$\mathbf{N}(\mathbf{x}) = \mathbf{N}(z_1, z_2, \ldots, z_p) = \mathbf{N}(\mathbf{z}) \tag{2}$$

where the z_i are linear combinations of the elements of $\mathbf{x}$, so that for some (p, n) transformation matrix, $\mathbf{T}_{\mathrm{N}}$,

$$\mathbf{z} = \mathbf{T}_{\mathrm{N}}\mathbf{x}. \tag{3}$$

The number of these co-ordinates, p, should be as small as possible, in which case $\mathbf{T}_{\mathrm{N}}$ will be rull rank.

The next step is to reduce the order of the model by using a reduction transformation derived from the linear part of the model. The transformation will be of the form

$$\mathbf{x} = \mathbf{T}\mathbf{q}, \tag{4}$$

where $\mathbf{q}$ is a vector of the r reduced co-ordinates and $\mathbf{T}$ is a transformation matrix of size (n, r), the form of which will be discussed later. Applying this transformation to equation (1), and premultiplying by the transpose of the transformation matrix, produces a set of r equations in the r generalized co-ordinates $\mathbf{q}$,

$$\mathbf{T}^{\mathrm{T}}\mathbf{M}\mathbf{T}\ddot{\mathbf{q}} + \mathbf{T}^{\mathrm{T}}\mathbf{D}\mathbf{T}\dot{\mathbf{q}} + \mathbf{T}^{\mathrm{T}}\mathbf{K}\mathbf{T}\mathbf{q} + \mathbf{T}^{\mathrm{T}}\mathbf{H}\mathbf{N}(\mathbf{z}) = \mathbf{T}^{\mathrm{T}}\mathbf{B}\mathbf{f}(t), \qquad \mathbf{y} = \mathbf{C}\mathbf{T}\mathbf{q}, \tag{5}$$

or, upon writing the transformed matrices and vectors with an overbar,

$$\bar{\mathbf{M}}\ddot{\mathbf{q}} + \bar{\mathbf{D}}\dot{\mathbf{q}} + \bar{\mathbf{K}}\mathbf{q} + \bar{\mathbf{H}}\mathbf{N}(\mathbf{z}) = \bar{\mathbf{B}}\mathbf{f}(t), \qquad \mathbf{y} = \bar{\mathbf{C}}\mathbf{q}. \tag{6}$$

The co-ordinates used to specify the non-linearity may be obtained from the reduced set of co-ordinates by combining equations (3) and (4) to give

$$\mathbf{z} = \mathbf{T}_{\mathrm{N}}\mathbf{T}\mathbf{q} = \bar{\mathbf{T}}_{\mathrm{N}}\mathbf{q}. \tag{7}$$

3. THE MODEL REDUCTION TECHNIQUES

Four model reduction techniques will be used to reduce the number of degrees-of-freedom in the linear system. It is assumed that the number of reduced degrees-of-freedom is greater than the number of degrees-of-freedom required to calculate the non-linearity, p. All the methods produce a reduced model that approximates the full model at the lower excitation frequencies. The first three reduction methods, described in this section, are based on the undamped part of the linear model; the reduction based on a balanced realization, described in the next section, includes damping. In the methods chosen, the transformations are applied once; methods that produce separate reduced models at different excitation frequencies in the harmonic balance method are not considered.

3.1. IMPROVED REDUCED SYSTEM (IRS)

O'Callahan [6] introduced this improvement on static reduction. The method provides a perturbation to the transformation from the static case by including the inertia terms as pseudo-static forces. The IRS transformation is based on choosing a subset of the co-ordinates as masters, to be retained, while the remaining co-ordinates are slaves which are eliminated. Thus

$$\mathbf{x} = \begin{Bmatrix} \mathbf{x}_{\mathrm{m}} \\ \mathbf{x}_{\mathrm{s}} \end{Bmatrix}, \qquad \text{where } \mathbf{q} \equiv \mathbf{x}_{\mathrm{m}} \tag{8}$$

and the subscripts m and s denote master and slave co-ordinates. The mass and stiffness matrices are partitioned based on the master and slave co-ordinates: for example,

$$\mathbf{M} = \begin{bmatrix} \mathbf{M}_{\mathrm{mm}} & \mathbf{M}_{\mathrm{ms}} \\ \mathbf{M}_{\mathrm{sm}} & \mathbf{M}_{\mathrm{ss}} \end{bmatrix}.$$

The transformation, $\mathbf{T}_{\mathrm{i}}$, is then given by

$$\mathbf{T}_{\mathrm{i}} = \mathbf{T}_{\mathrm{s}} + \mathbf{S}\mathbf{M}\mathbf{T}_{\mathrm{s}}\mathbf{M}_{\mathrm{R}}^{-1}\mathbf{K}_{\mathrm{R}}, \tag{9}$$

where

$$\mathbf{S} = \begin{bmatrix} \mathbf{0} & \mathbf{0} \\ \mathbf{0} & \mathbf{K}_{\mathrm{ss}}^{-1} \end{bmatrix}$$

and $\mathbf{T}_{\mathrm{s}}$ is the transformation obtained from static reduction [7], given by

$$\mathbf{T}_{\mathrm{s}} = \left[\frac{\mathbf{I}}{-\mathbf{K}_{\mathrm{ss}}^{-1}\mathbf{K}_{\mathrm{sm}}} \right] \tag{10}$$

$\mathbf{M}_R$ and $\mathbf{K}_R$ are the following reduced mass and stiffness matrices, obtained from static reduction,

$$\mathbf{M}_R = \mathbf{T}_s^T \mathbf{M} \mathbf{T}_s, \qquad \mathbf{K}_R = \mathbf{T}_s^T \mathbf{K} \mathbf{T}_s. \tag{11}$$

Automatic methods to choose the master-degrees-of-freedom are available based on static reduction: for example, the method of Henshell and Ong [8, 9]. Friswell *et al*. [10] outlined an iterated IRS method, in which the improved reduced matrices $\mathbf{M}_R$ and $\mathbf{K}_R$ are used in equation (9). On convergence the reduced model produces the SEREP transformation described below.

3.2. SYSTEM EQUIVALENT REDUCTION EXPANSION PROCESS (SEREP)

In this reduction [11] the computed eigenvectors are used to produce the transformation between the master and slave co-ordinates. The matrix containing the first r analytical eigenvectors, Φ, is partitioned into the master and slave co-ordinates. When the number of master co-ordinates is greater than the number of modes then

$$\mathbf{T}_u = \begin{bmatrix} \Phi_m \\ \hline \Phi_s \end{bmatrix} \Phi_m^+, \qquad \text{where } \Phi_m^+ = (\Phi_m^T \Phi_m)^{-1} \Phi_m^T \tag{12}$$

and Φ_m and Φ_s are the parts of the analytical eigenvectors associated with the master and slave co-ordiantes respectively. When this method is used the reduced model will exactly reproduce the lower natural frequencies of the full linear model.

3.3. MODAL COORDINATES

The SEREP reduction method reproduces the lower modes of the linear system. An alternative is to transform the equations into modal co-ordinates. The reduced co-ordinates are now modal participation factors rather than specified physical co-ordinates. The transformation matrix is the first r columns of the eigenvector matrix

$$\mathbf{T}_m = \Phi. \tag{13}$$

4. CONTROLLABILITY, OBSERVABILITY AND BALANCED REALIZATIONS

The concepts of controllability and observability originated in Control Engineering. In simple terms, a system is controllable if an input exists that enables the states of the system to attain any arbitrary value. Similarly a system is observable if the states of the system may be deduced from the output. The determination of system controllability and observability is usually based on the state representation of the system although it is possible to work directly with the second order equations of motion [12].

Equation (1) may be written as

$$\frac{d}{dt}\begin{Bmatrix} \mathbf{x} \\ \dot{\mathbf{x}} \end{Bmatrix} = \begin{bmatrix} \mathbf{0} & \mathbf{I} \\ -\mathbf{M}^{-1}\mathbf{K} & -\mathbf{M}^{-1}\mathbf{D} \end{bmatrix}\begin{Bmatrix} \mathbf{x} \\ \dot{\mathbf{x}} \end{Bmatrix} + \begin{bmatrix} \mathbf{0} \\ -\mathbf{M}^{-1}\mathbf{H} \end{bmatrix}\mathbf{N}(\mathbf{z}) + \begin{bmatrix} \mathbf{0} \\ \mathbf{M}^{-1}\mathbf{B} \end{bmatrix}\mathbf{f}(t),$$

$$\mathbf{y} = [\mathbf{C} \quad \mathbf{0}]\begin{Bmatrix} \mathbf{x} \\ \dot{\mathbf{x}} \end{Bmatrix}, \tag{14}$$

where

$$\mathbf{z} = [\mathbf{T}_{\mathrm{N}} \quad \mathbf{0}]\begin{Bmatrix}\mathbf{x}\\ \dot{\mathbf{x}}\end{Bmatrix}.$$

Equation (14) may be rewritten in terms of the state vector, $\mathbf{w}$, as

$$\dot{\mathbf{w}} = \mathbf{A}\mathbf{w} + \hat{\mathbf{H}}\mathbf{N}(\mathbf{z}) + \hat{\mathbf{B}}\mathbf{f}(t), \qquad \mathbf{y} = \hat{\mathbf{C}}\mathbf{w}, \tag{15}$$

where

$$\mathbf{z} = \hat{\mathbf{T}}_{\mathrm{N}}\mathbf{w}, \qquad \mathbf{w} = \begin{Bmatrix}\mathbf{x}\\ \dot{\mathbf{x}}\end{Bmatrix}$$

and the matrix definitions may be deduced by comparing equations (14) and (15). The controllability and observability grammians for the linear part of equation (15), $\mathbf{W}_c$ and $\mathbf{W}_o$ respectively, are defined for a stable, time invariant system as

$$\mathbf{W}_c = \int_0^\infty e^{\mathbf{A}\tau}\,\hat{\mathbf{B}}\hat{\mathbf{B}}^{\mathrm{T}}\,e^{\mathbf{A}^{\mathrm{T}}\tau}\,d\tau, \qquad \mathbf{W}_o = \int_0^\infty e^{\mathbf{A}^{\mathrm{T}}\tau}\,\hat{\mathbf{C}}^{\mathrm{T}}\hat{\mathbf{C}}\,e^{\mathbf{A}\tau}\,d\tau. \tag{16, 17}$$

These grammians are conveniently calculated from the algebraic Lyapunov equations [12–14],

$$\mathbf{A}\mathbf{W}_c + \mathbf{W}_c\mathbf{A}^{\mathrm{T}} + \hat{\mathbf{B}}\hat{\mathbf{B}}^{\mathrm{T}} = \mathbf{0}, \qquad \mathbf{A}^{\mathrm{T}}\mathbf{W}_o + \mathbf{W}_o\mathbf{A} + \hat{\mathbf{C}}^{\mathrm{T}}\hat{\mathbf{C}} = \mathbf{0}. \tag{18, 19}$$

The grammians are positive semi-definite, and for a controllable and observable system are positive definite. If a system is controllable and observable then a useful measure is how close the grammians are to being rank deficient: that is, how close the system is to being uncontrollable or unobservable. This measure takes the form of the ratio of the largest to the smallest singular value of the grammians.

Moore [14] introduced the idea of a balancing transformation. The state of the system is transformed so that the controllability and observability grammians are diagonal and equal. Laub [13] gave an efficient method for the calculation of this transformation, which is implemented in MATLAB [15]. If $\mathbf{T}_b$ is the balancing transformation then equation (15) becomes

$$\dot{\mathbf{v}} = \tilde{\mathbf{A}}\mathbf{v} + \tilde{\mathbf{H}}\mathbf{N}(\mathbf{z}) + \tilde{\mathbf{B}}\mathbf{f}(t), \qquad \mathbf{y} = \tilde{\mathbf{C}}\mathbf{v}, \tag{20}$$

where

$$\mathbf{w} = \mathbf{T}_b\mathbf{v}, \qquad \tilde{\mathbf{A}} = \mathbf{T}_b^{-1}\mathbf{A}\mathbf{T}_b, \qquad \tilde{\mathbf{H}} = \mathbf{T}_b^{-1}\hat{\mathbf{H}}, \qquad \tilde{\mathbf{B}} = \mathbf{T}_b^{-1}\hat{\mathbf{B}}, \qquad \tilde{\mathbf{C}} = \hat{\mathbf{C}}\mathbf{T}_b.$$

The model may be reduced by eliminating those transformed states that are least controllable and observable [12, 14]. The reduced matrices are calculated by using an approach similar to static reduction in dynamics. If $\mathbf{v}_m$ represents those states which are retained, $\mathbf{v}_s$ those that are eliminated, and the matrices $\tilde{\mathbf{A}}$, $\tilde{\mathbf{H}}$, $\tilde{\mathbf{B}}$ and $\tilde{\mathbf{C}}$ are partitioned accordingly, then the reduced model is

$$\dot{\mathbf{v}}_m = [\tilde{\mathbf{A}}_{mm} - \tilde{\mathbf{A}}_{ms}\tilde{\mathbf{A}}_{ss}^{-1}\tilde{\mathbf{A}}_{sm}]\mathbf{v}_m + [\tilde{\mathbf{H}}_m - \tilde{\mathbf{A}}_{ms}\tilde{\mathbf{A}}_{ss}^{-1}\tilde{\mathbf{H}}_s]\mathbf{N}(\mathbf{z}) + [\tilde{\mathbf{B}}_m - \tilde{\mathbf{A}}_{ms}\tilde{\mathbf{A}}_{ss}^{-1}\tilde{\mathbf{B}}_s]\mathbf{f}(t),$$

$$\mathbf{y} = [\tilde{\mathbf{C}}_m - \tilde{\mathbf{C}}_s\tilde{\mathbf{A}}_{ss}^{-1}\tilde{\mathbf{A}}_{sm}]\mathbf{v}_m - \tilde{\mathbf{C}}_s\tilde{\mathbf{A}}_{ss}^{-1}\tilde{\mathbf{B}}_s\mathbf{f}(t), \tag{21}$$

where

$$\mathbf{v} = \begin{Bmatrix} \mathbf{v}_m \\ \mathbf{v}_s \end{Bmatrix}, \qquad \tilde{\mathbf{A}} = \begin{bmatrix} \tilde{\mathbf{A}}_{mm} & \tilde{\mathbf{A}}_{ms} \\ \tilde{\mathbf{A}}_{sm} & \tilde{\mathbf{A}}_{ss} \end{bmatrix}, \qquad \tilde{\mathbf{H}} = \begin{bmatrix} \tilde{\mathbf{H}}_m \\ \tilde{\mathbf{H}}_s \end{bmatrix},$$

$$\tilde{\mathbf{B}} = \begin{bmatrix} \tilde{\mathbf{B}}_m \\ \tilde{\mathbf{B}}_s \end{bmatrix}, \qquad \tilde{\mathbf{C}} = [\tilde{\mathbf{C}}_m \quad \tilde{\mathbf{C}}_s].$$

In generating equation (21) from equation (20), $\dot{\mathbf{v}}_s$ is assumed to be zero, and the reduction is similar to that for a linear system, except that the non-linear distribution matrix, $\tilde{\mathbf{H}}$, must also be reduced. For lightly damped linear, elastic structures the resulting transformation is often very similar to the reduction to modal co-ordinates. One difficulty is that the co-ordinates specifying the non-linearity, $\mathbf{z}$, must be calculated. The transformation given by equation (21) suggests that this estimator should be given by

$$\mathbf{z} = \hat{\mathbf{T}}_N \mathbf{T}_b \begin{bmatrix} \mathbf{I} \\ -\tilde{\mathbf{A}}_{ss}^{-1} \tilde{\mathbf{A}}_{sm} \end{bmatrix} \mathbf{v}_m + \hat{\mathbf{T}}_N \mathbf{T}_b \begin{bmatrix} \mathbf{0} \\ -\tilde{\mathbf{A}}_{ss}^{-1} \tilde{\mathbf{B}}_s \end{bmatrix} \mathbf{f} + \hat{\mathbf{T}}_N \mathbf{T}_b \begin{bmatrix} \mathbf{0} \\ -\tilde{\mathbf{A}}_{ss}^{-1} \tilde{\mathbf{H}}_s \end{bmatrix} \mathbf{N}(\mathbf{z}). \tag{22}$$

Equation (22) is an implicit function in $\mathbf{z}$, which complicates the analysis of the reduced system. Also the results obtained by using this estimator are poor, and far better results are obtained by using the simplified estimator

$$\mathbf{z} = \hat{\mathbf{T}}_N \mathbf{T}_b \begin{bmatrix} \mathbf{I} \\ \mathbf{0} \end{bmatrix} \mathbf{v}_m. \tag{23}$$

The reduction transformation is based on the observability and controllability of the linear part of the model. To allow for a local non-linearity, the co-ordinates used to specify the non-linearity, given by the transformation equation (3), should be included in the output matrix, $\mathbf{C}$. Generally the force produced by the local non-linearity will occur only at a limited number of combinations of degrees-of-freedom, given by the matrix $\mathbf{H}$ in equation (1). These force locations should be included in the input matrix, $\mathbf{B}$. For example, a non-linear translational spring will produce a force which is a function of the spring extension. The force produced by the spring will occur at its two ends, and the forces will be equal in magnitude but opposite in direction. Therefore in the computation of the reduction transformation one extra input and one extra output is specified. Once the reduction transformation has been calculated, these extra inputs and outputs are neglected.

5. USING THE REDUCED MODEL TO CALCULATE THE RECEPTANCE

The receptance will be calculated by using the harmonic balance method. The response of each degree-of-freedom is assumed to be at the excitation frequency only, although not necessarily in phase with the force or with the response of any other degree-of-freedom. Other more accurate methods are available to estimate the structure's receptance [16–21], although this form of the harmonic balance method will serve our purpose here to look at the inaccuracies introduced by the model reduction. Friswell and Penny [22] showed that, for a single-degree-of-freedom system with a cubic non-linearity, the error in the jump frequency and the error in the magnitude just before the jump is small for a large range of forcing magnitudes and damping values. For multi-degree-of-freedom systems the situation is more complex. The errors may be large if any of the neglected harmonics coincides with the higher natural frequencies of the system or if combination type resonances are excited.

The approximate response at the excitation frequency is obtained by neglecting terms that are harmonics of the excitation frequency. For a single-degree-of-freedom system this produces a cubic polynomial for the response magnitude [22, 23]. For a multi-degree-of-freedom case each degree-of-freedom, x_i, is written as

$$x_i = A_i \cos \omega t + B_i \sin \omega t, \tag{24}$$

for some constants A_i and B_i. Substituting these expressions for the system response into the equations of motion for a cubic stiffening non-linearity gives a set of simultaneous cubic polynomials in the constants A_i and B_i. These non-linear simultaneous equations may be solved by using the Newton-Raphson method with the initial values taken to be the parameters from the previous frequency. Using this choice of initial values simulates an experiment where the excitation frequency is either swept up or down.

6. THE RECEPTANCE OF A CANTILEVER BEAM SYSTEM

Figure 1 shows the example of two cantilever beams whose free ends are joined by a discrete linear and cubic stiffening spring and also by a damper. Each cantilever is discretized into six elements, giving 12-degrees-of-freedom per beam, or 24 altogether. The structure is assumed to be forced at degree-of-freedom 7 and the response measured at degree-of-freedom 17, as marked on Figure 1. The system is excited with a sinusoidal force of 250 N around the second resonance at approximately 301 rad/s. Note that the second linear natural frequency is approximately 262 rad/s.

6.1. IRS REDUCTION

Figure 2 shows the receptance of the full model during an upward frequency sweep between 270 rad/s and 330 rad/s. Also shown are the effects of using reduced models with four-degrees-of-freedom, based on the IRS method with different sets of reduced co-ordinates. The quality of the receptance depends on the choice of master co-ordinates, and clearly demonstrates the need to choose these co-ordinates very carefully. Table 1 shows the estimated jump frequencies for each set of degrees-of-freedom. Table 2 shows the natural frequencies of the linear part of the reduced model, to give some idea of the accuracy of the IRS reduction. The set of co-ordinates 5, 9, 15, 19 is the one chosen by the automatic selection procedure based on static reduction, where all the degrees-of-freedom are possible master co-ordinates [9]. The results follow the expected trend; as the retained-, or master-degrees-of-freedom, become more remote from the non-linearity, the resulting receptance becomes less accurate. The results for

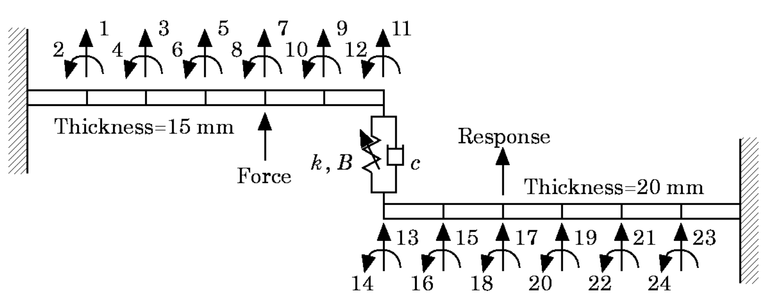

Figure 1. The twin cantilever beam example (24-degrees-of-freedom). $k = 10\,\text{kN/m}$, $B = 2\,\text{MN/m}^3$, $c = 10\,\text{Ns/m}$, $E = 70\,\text{GN/m}^2$, $\rho = 2700\,\text{kg/m}^3$.

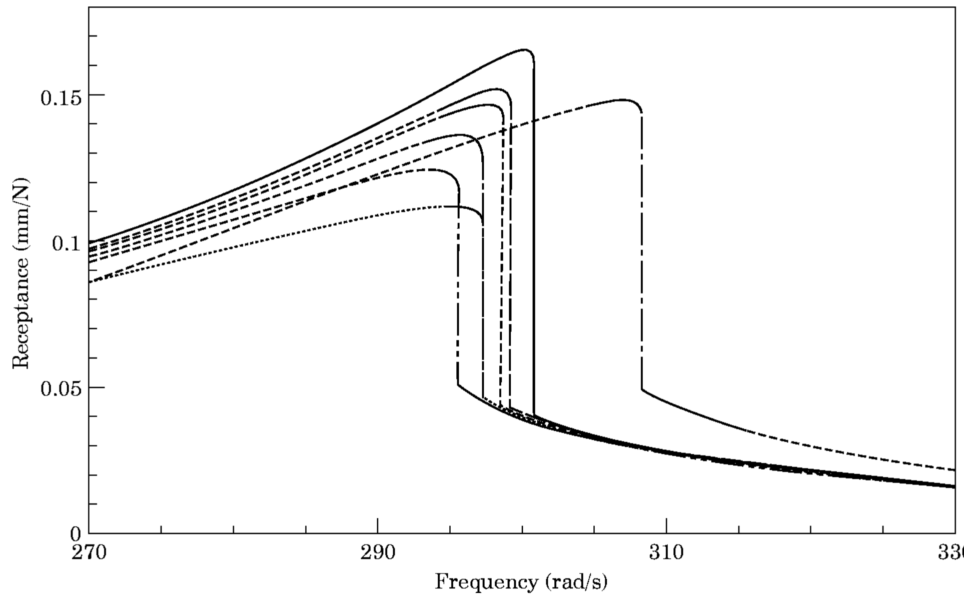

Figure 2. Results of IRS reduction for the twin cantilever beam example; the effect of the choice of master d.o.f. on the receptance near the second resonance. ——, No reduction. D.o.f.: – – – –, 11, 12, 13, 14; - - - - -, 7, 11, 13, 17; – · – · –, 5, 9, 15, 19; – ·· – ·· –, 5, 6, 19, 20; · · · · · · ·, 5, 6, 11, 12; —————, 1, 2, 3, 4.

degrees-of-freedom 5, 6, 11, 12 and 1, 2, 3, 4 are particularly bad because the master co-ordinates are located on only one beam. The estimation of the extension in the non-linear spring is likely to be poor in these cases. In the case of degrees of freedom 1, 2, 3, 4, even the estimate of the response at the tip of the thinner beam is likely to be poor.

6.2. REDUCTION TO MODAL CO-ORDINATES AND SEREP

Figure 3 shows the results of reducing the model to 4, 5 or 6 modal co-ordinates. The results for SEREP are identical, providing a really poor choice of co-ordinates is not chosen (which would result in a poorly conditioned pseudo-inverse in equation (12)). The results follow the expected trend, in that the more modes that are used, the more accurate

TABLE 1

Twin cantilever beam example results obtained by using IRS reduction: jump frequencies and linear natural frequencies

		Natural frequencies (rad/s)			
Reduced DoF set	Jump frequency (rad/s)	1	2	3	4
No reduction	300·6	92·714	261·97	536·65	682·68
11, 12, 13, 14	299·1	92·714	261·82	539·01	683·03
7, 11, 13, 17	298·5	92·714	261·77	537·45	681·65
5, 9, 15, 19	297·1	92·714	261·65	535·82	681·15
5, 6, 19, 20	295·4	92·714	261·40	538·40	688·01
5, 6, 11, 12	297·2	92·714	261·79	540·37	1401·86
1, 2, 3, 4	308.2	92·734	279·31	819·64	3960·76

TABLE 2

Jump frequencies for the twin cantilever beam example obtained by using reduction to modal co-ordinates

No. of modes	Jump frequency (rad/s)
No reduction	300·6
7	300·4
6	300·0
5	299·5
4	297·3

the reduced model. Interestingly, using four modal co-ordinates is not as accurate as model reduction based on the IRS method and the best choice of master co-ordinates.

6.3. REDUCTION VIA A BALANCED REALISATION

Figure 4 shows the results of reducing the model using observability and controllability considerations, via the balanced realisation approach. Reduction to 14, 12, 10 and 8 states is performed, which is equivalent to 7, 6, 5 and 4 modes in the reduction to modal co-ordinates method, since each mode may be represented by two states. To obtain the reduction transformation the displacement output and the extension in the non-linear spring are used as the two system outputs. Similarly the actual force input and the force produced by the non-linear spring are used as the two inputs. Table 3 shows the jump frequencies and the first four natural frequencies of the reduced model. The results follow the expected trend, in that the more states that are used, the more accurate is the reduced model. Using eight states produces a more accurate receptance than either reduction to four modal co-ordinates, or reduction by IRS with the best choice of master co-ordinates.

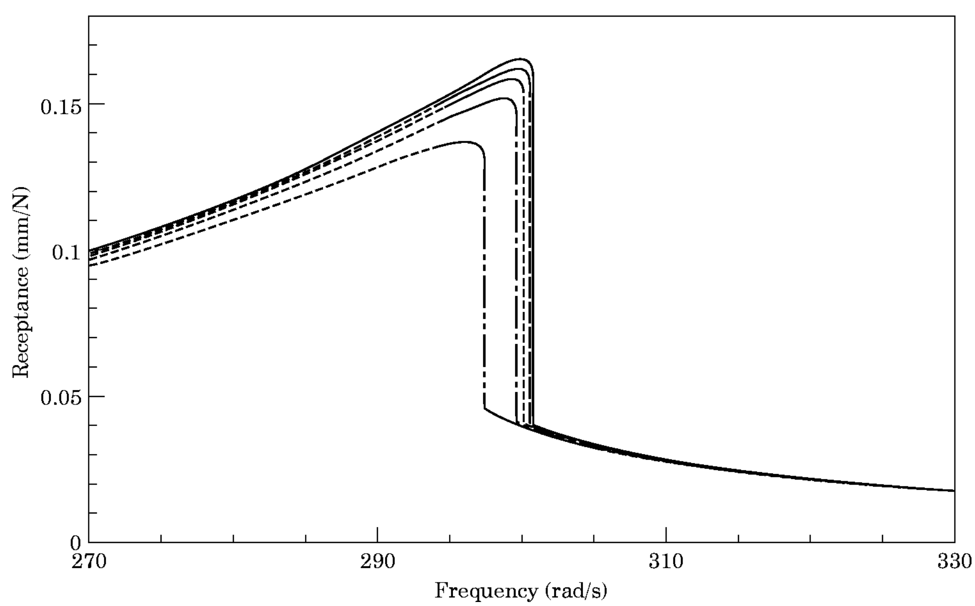

Figure 3. Results of reduction to modal co-ordinates for the twin cantilever beam example; the effect of the number of modes retained on the receptance near the second resonance. ——, No reduction; – – – –, 7 modes; - - - - -, 6 modes; – · – · –, 5 modes; – ·· – ·· –, 4 modes.

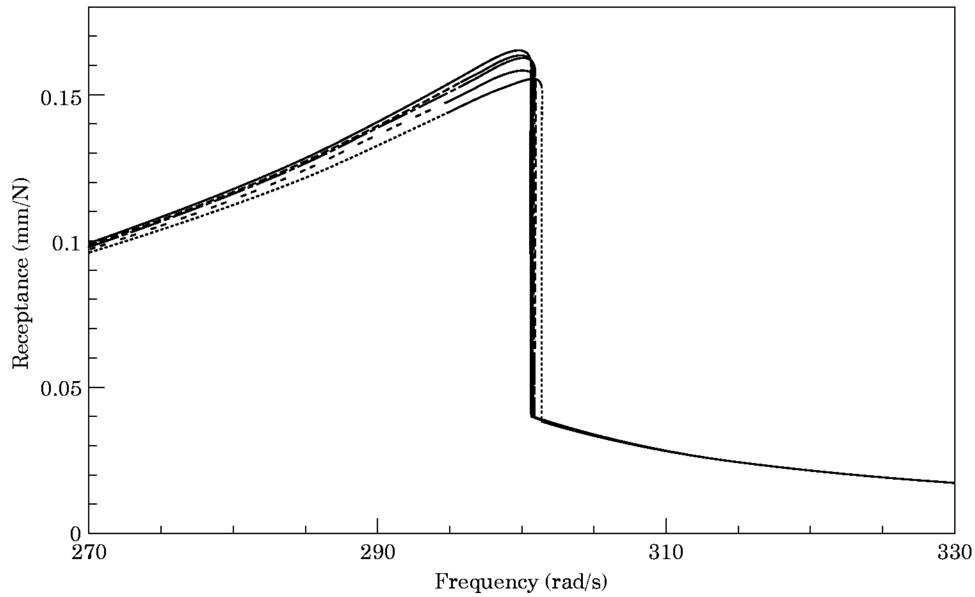

Figure 4. Results of reduction based on observability, controllability and balanced realizations for the twin cantilever beam example; the effect of the number of states retained on the receptance near the second resonance. Number of states: ——, No reduction; – – – –, 14; – ·· – ·· –, 12; - - - - -, 10; · · · · · · ·, 8.

7. A POINCARÉ MAP OF A PINNED BEAM SYSTEM

Figure 5 shows a beam that is pinned at both ends and is forced at its centre. Backlash, or clearance, is modelled in the system by including stiff springs at the mid point with a clearance of 0·005 m. Lin and Ewins [24] considered the equivalent one-degree-of-freedom case of this example in depth and also considered a two-degree-of-freedom discrete example. This model also has applications in the analysis of rotor systems and has been used to model subharmonic response of a rotor [25]. Similar models may be used to simulate the dynamics of cracked beams or shafts. The system shown has the excitation and the non-linear stops at the same location. This is not a constraint of the method but it does mean the model may be reduced to a single-degree-of-freedom easily. The beam is modelled with 8 beam elements giving 16-degrees-of-freedom. The symmetry in the model implies that the even modes of the beam will not be excited. The time response of the model is calculated by using a Runge-Kutta fourth order integration scheme with a step length varied to given a uniform solution accuracy. Friswell *et al*. [3] demonstrated

TABLE 3

Jump frequencies for the twin cantilever beam example obtained by using reduction based on observability, controllability and balanced realizations

No. of states	Jump frequency (rad/s)	Natural frequencies (rad/s) 1	2	3	4
No reduction	300·6	92·714	261·97	536·65	682·68
14	300·7	92·714	261·97	536·65	682·71
12	300·8	92·714	261·97	536·66	682·77
10	300·9	92·714	261·98	536·71	683·19
8	301·4	92·714	261·99	537·07	685·07

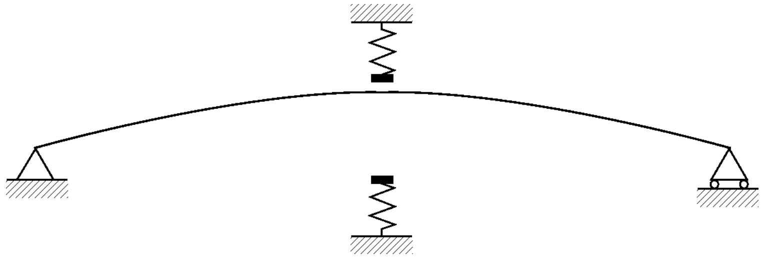

Figure 5. The pinned beam example (16-degrees-of-freedom). Flexural rigidity $EI = 7.8750$ N m^2; mass/unit length = 0.4050 kg/m; beam length = 1 m; proportional damping $\mathbf{C} = \alpha\mathbf{M} + \beta\mathbf{K}$, $\alpha = 5$, $\beta = 10^{-5}$; discrete spring constant = 20 kN/m.

the inaccuracies introduced by reducing the linear part of the model using the SEREP method. Here the reduction of the linear part by using reduction to modal co-ordinates and by using balanced realizations, respectively, will be compared.

Figure 6 shows the Poincaré map of this system, excited at 40 Hz with a magnitude of 40 N, calculated by using the full set of 16-degrees-of-freedom. The differential equations were integrated for 20 000 cycles, which is equivalent to 500 seconds, and the first 1000 points were discarded when the Poincaré maps were plotted. The section of the map considered has the excitation at the forcing location along the x-axis and the corresponding velocity on the y-axis. The map shows a fuzzy collection of points which is typical of high order chaotic systems. The strange attractor must be viewed in the full 32 dimensional phase space to appreciate fully the implicit order in the system.

7.1. REDUCTION TO MODAL CO-ORDINATES

Reducing the model of the beam to five modes, which is equivalent to reduction to the first three odd modes, produces a Poincaré map that is very similar to Figure 6. Thus a

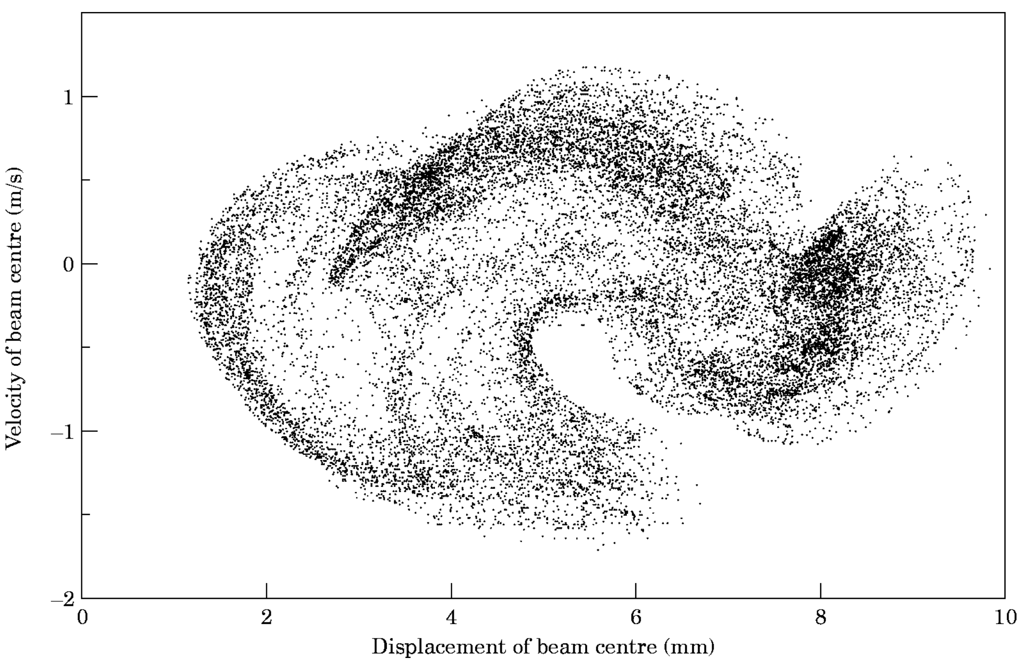

Figure 6. Poincaré map for the pinned beam with 16 d.o.f.

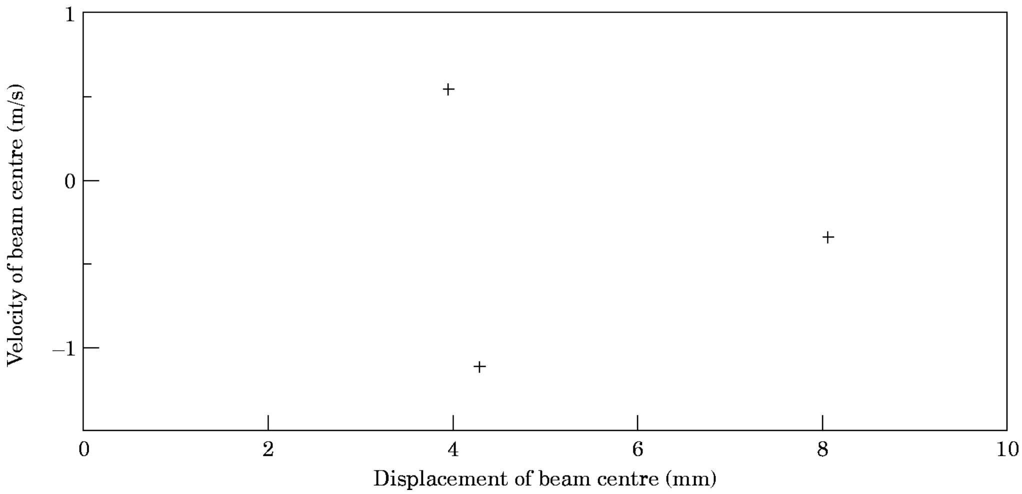

Figure 7. As Figure 6 but model reduced to the three lowest frequency modal co-ordinates.

reduced system with three-degrees-of-freedom, namely the first three odd modal co-ordinates, could replace the full system with only a limited loss of accuracy.

Reducing the number of modes to three, that is the first two odd modes, changes the character of the dynamics to a periodic motion with period three times that of the excitation, shown in Figure 7. Obviously the model has been reduced too far and the character of the resulting dynamics has changed. Initially the dynamics look chaotic but settle into the period three orbit after a time which is dependent on the accuracy of the solution. The smaller the accuracy tolerance the faster the periodic motion begins. The dynamics of the system is close to the boundary between chaotic and periodic motion and small changes, due to the model reduction or errors in the numerical integration, can force the dynamics over this boundary.

Finally, if the model is reduced to a single modal co-ordinate the Poincaré map shown in Figure 8 is obtained. Since the phase space now has dimension two one can view the whole space. The character of the attractor is completely different to those found with a higher number of degrees-of-freedom. Figures 6–8 are equivalent to those obtained by using the SEREP reduction method, as would be expected providing the retained coordinates in the SEREP are chosen well. Reduction to modal co-ordinates has the advantage, in this example, in that the even modes may be easily eliminated, producing a reduced model of lower order.

7.2. REDUCTION VIA A BALANCED REALIZATION

Reduction of the linear part of the model to a sixth order system using the balanced realization approach outlined in Section 4, equivalent in model size to three odd modes, produces a Poincaré map that is very similar to Figure 6. The reduction transformation is obtained by assuming the input is the force applied at the centre of the beam, and the outputs are the displacement and velocity at the centre of the beam. The even modes are both uncontrollable and unobservable when using this set of inputs and outputs, and therefore will have no effect on the reduction. The output, or measurement, matrix produced the displacement and velocity at the beam centre. Thus the reduced system introduces only a limited loss of accuracy. Reduction to a fourth order system, equivalent in model size to two odd modes, produces the Poincaré map shown in Figure 9. The character of the plot is very similar to that of the full system, although close inspection

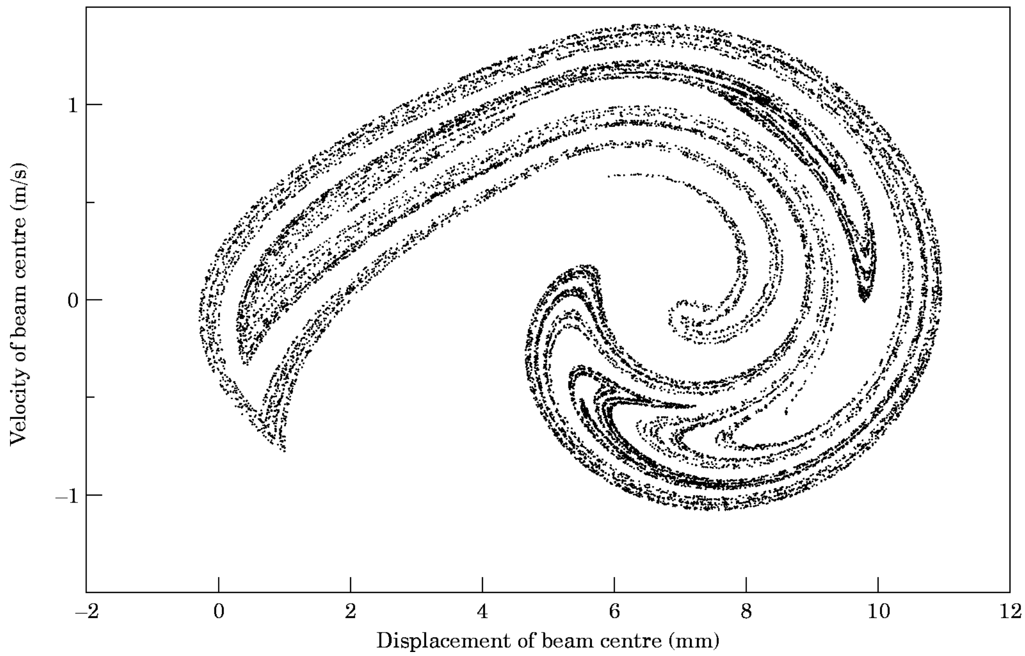

Figure 8. As Figure 6 but model reduced to the lowest frequency modal co-ordinate.

reveals that the attractor is rotated slightly, and the distributions of density of the points are slightly different. Even so the model predicts a chaotic response that is close to that of the full system, and certainly better than the periodic response predicted by reduction to modal co-ordinates, shown in Figure 7. Figure 10 shows the reduction of the linear part

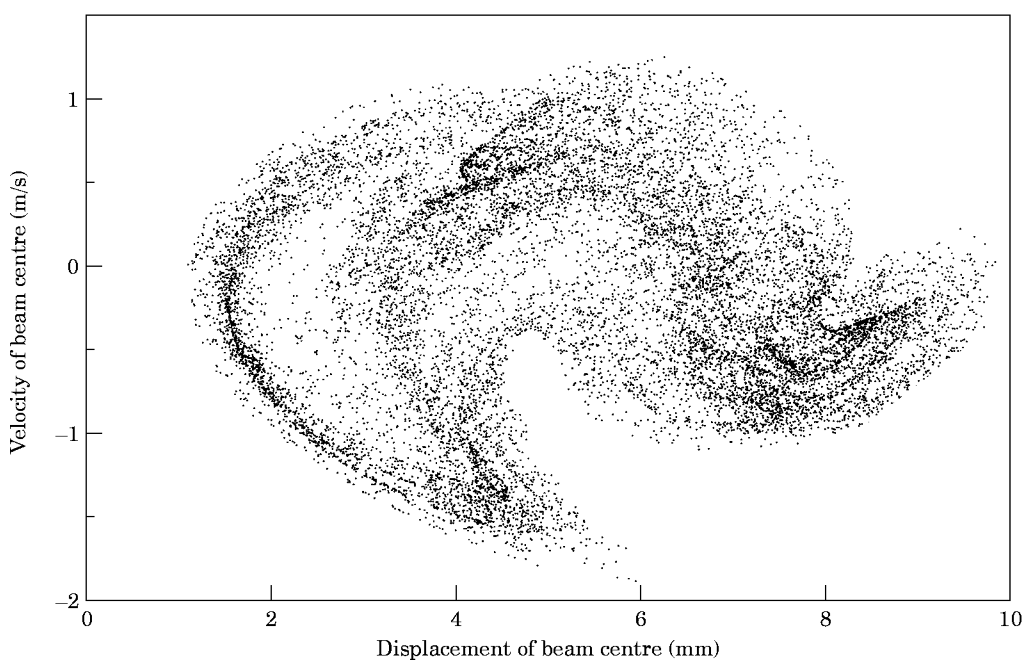

Figure 9. As Figure 6 but model reduced to a fourth order system by using a balanced realization.

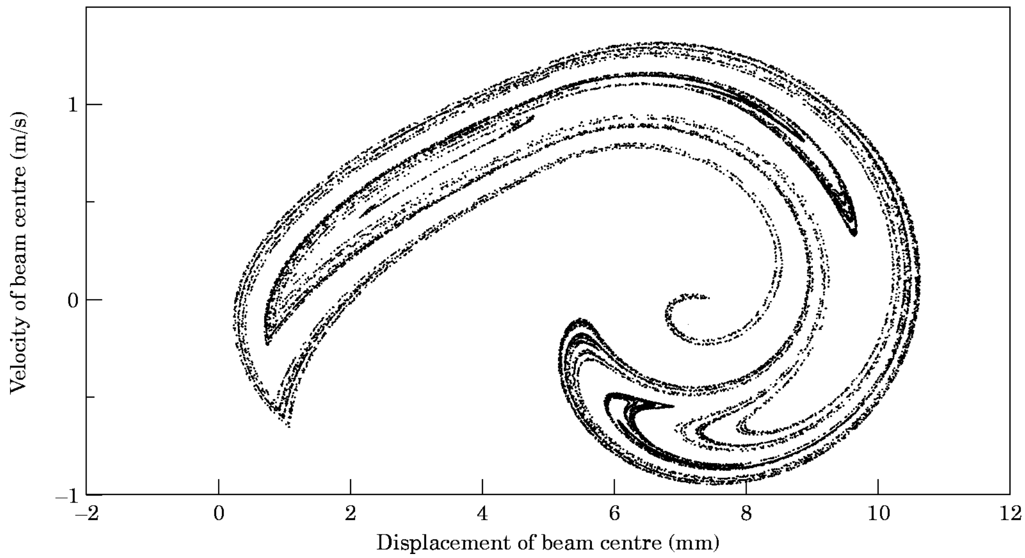

Figure 10. As Figure 6 but model reduced to a second order system by using a balanced realization.

of the model to a second order system by using the balanced realization approach, which is equivalent in model size to reduction to a single mode. The attractor is very similar to that obtained by reduction to a single modal co-ordinate, although there are differences in the minor features of the attractor. Table 4 shows the natural frequencies and damping ratios for these reduced models, and demonstrates that the reduction by using a balanced realization gives a reduced order system which closely reproduces the lower modes.

8. CONCLUSIONS

The application of model reduction techniques for linear systems to structures with non-linear components has been considered. The methods have been tested by calculating the receptance of a system consisting of two cantilever beams joined with a cubic spring. When using the IRS method the master-degrees-of-freedom should be chosen carefully to produce an accurate reduced model. Better quality results are obtained if the co-ordinates required to specify the non-linearity are retained after the reduction. Reduction to modal co-ordinates is easy to apply and gives acceptable results, although a more accurate

TABLE 4

Natural frequencies and damping ratios for the pinned beam example obtained by using reduction based on observability, controllability and balanced realizations

No. of states	Natural frequencies (ω_i, rad/s) and damping ratios (ζ_i, %)					
	ω_1	ζ_1	ω_2	ζ_2	ω_3	ζ_3
No reduction	43·522	5·7660	392·19 (mode 3)	0·8335	1098·1 (mode 5)	0·7767
6	43·521	5·7660	392·18	0·8335	1097·9	0·7767
4	43·520	5·7659	392·17	0·8332		
2	43·515	5·7658				

reduced model may be obtained with IRS and the best choice of master co-ordinates. Reduction based on observability and controllability considerations, via balanced realizations, gives the best results, although implementing such a reduction method requires more computation initially. The reduction to modal co-ordinates and reduction based on balanced realizations were tested for time domain analysis by calculating the Poincaré map of a pinned beam with clearance. The balanced realization approach gave more accurate results for these simulations.

The effect of linear model reduction on examples of non-linear systems has been considered in this paper. Some general conclusions may be drawn, although the reduction of a specific system should always be handled with care. Although IRS reduction sometimes performs well, a suitable set of master co-ordinates must be chosen. Balanced realizations appear to offer a rational method to apply model reduction. Although the computation required is considerable for a linear system, it is small in comparison with the computation of the non-linear response. Therefore the balanced realization approach may be computationally efficient. Producing the equations in state space form is not a disadvantage, as the subsequent analysis, for example time integration schemes, often requires a first order set of differential equations.

REFERENCES

1. A. D. Dimarogonas and C. A. Papadopoulos 1983 *Journal of Sound and Vibration* **91**, 583–593. Vibration of cracked shafts in bending.
2. L. Changhe, O. Bernasconi and N. Xenophontidis 1989 *Transactions of the ASME Journal of Vibration, Acoustics, Stress and Reliability in Design* **111**, 257–263. A generalized approach to the dynamics of cracked structures.
3. M. I. Friswell, J. E. T. Penny and S. D. Garvey 1995 *Mechanical Systems and Signal Processing* **9**, 317–328. Using linear model reduction to investigate the dynamics of structures with local non-linearities.
4. S.-C. Wu and E. J. Haug 1988 *International Journal for Numerical Methods in Engineering* **26**, 2211–2226. Geometric non-linear substructuring for dynamics of flexible mechanical systems.
5. C.-H. Sheu, G. De Roeck, M. Van Laethem and P. Geyskens 1990 *Computers and Structures* **35**, 593–601. Application of the substructuring technique to non-linear dynamic structural analysis.
6. J. C. O'Callahan 1989 *7th IMAC*, 17–21. A procedure for an improved reduced system (IRS) model.
7. R. J. Guyan 1965 *AIAA Journal* **3**, 380. Reduction of stiffness and mass matrices.
8. R. D. Henshall and J. H. Ong 1975 *International Journal of Earthquake and Structural Dynamics* **3**, 375–383. Automatic masters for eigenvalue economisation.
9. J. E. T. Penny, M. I. Friswell and S. D. Garvey 1994 *AIAA Journal* **32**, 407–414. The automatic choice of measurement locations for dynamic tests.
10. M. I. Friswell, S. D. Garvey and J. E. T. Penny 1995 *Journal of Sound and Vibration* **186**, 311–323. Model reduction using dynamic and iterated IRS techniques.
11. J. O'Callahan, P. Avitabile and R. Riemer 1989 *7th IMAC*, 29–37. System equivalent reduction expansion process.
12. R. E. Skelton 1988 *Dynamic Systems Control, Linear Systems Analysis and Synthesis*. New York: John Wiley & Sons.
13. A. J. Laub 1980 *ASME Joint Automatic Control Conference, Paper* FA8-E. Computation of 'balancing' transformations.
14. B. Moore 1981 *IEEE Transactions on Automatic Control* **AC-26**, 17–32. Principal component analysis in linear systems: controllability, observability, and model reduction.
15. Mathworks Inc. 1994 *Control System Toolbox User's Guide*.
16. H. Tamura, T. Kondou and A. Sueoka 1986 *Bulletin of the Japanese Society of Mechanical Engineers* **29**, 894–901. Higher approximate solutions of the Duffing equation (odd order superharmonic resonances in the hard spring system).

17. Y. TSUDA, J. INOUE, H. TAMURA and A. SUEOKA 1984 *Bulletin of the Japanese Society of Mechanical Engineers* **27**, 1280–1287. On the 1/2-th subharmonic vibrations of a non-linear vibrating system with a hard Duffing type restoring characteristic.
18. S. L. LAU and Y. K. CHEUNG 1981 *Journal of Applied Mechanics* **48**, 959–964. Amplitude incremental variational principle for non-linear vibration of elastic systems.
19. A. A. FERRI 1986 *Transactions of the ASME*, *Journal of Applied Mechanics* **53**, 455–457. On the equivalence of the incremental harmonic balance method and the harmonic balance-Newton-Raphson method.
20. Y. K. CHEUNG and V. P. IU 1988 *Engineering Computations* **5**, 134–140. An implicit implementation of harmonic balance method for non-linear dynamic systems.
21. E. BUDAK and H. ÖZGÜVEN 1993 *Mechanical Systems and Signal Processing* **7**, 75–87. Iterative receptance method for determining harmonic response of structures with symmetrical non-linearities.
22. M. I. FRISWELL and J. E. T. PENNY 1994 *Journal of Sound and Vibration* **169**, 261–269. The accuracy of jump frequencies in series solutions of the response of a Duffing oscillator.
23. D. W. JORDAN and P. SMITH 1977 *Non-linear Ordinary Differential Equations*. Oxford University Press.
24. R. M. LIN and D. J. EWINS 1993 *Mechanical Systems and Signal Processing* **7**, 257–272. Chaotic vibration of mechanical systems with backlash.
25. F. F. EHRICH 1988 *Transactions of the ASME Journal of Vibration*, *Acoustics*, *Stress and Reliability in Design* **110**, 9–16. High order subharmonic response of high speed rotors in bearing clearance.